REPORT DOCUMENTATION PAGE

AFRL-SR-AR-TR-04-

0152

1. REPORT DATE (DD-MM-YYYY)	2. REPORT TYPE	3. DATES COVERED (From - To)
24-02-2004	Final Report	12-01-2000 to 11-30-2003

4. TITLE AND SUBTITLE
Residual Stresses in Thermosetting Resins for Polymer Matrix Composites: Modeling and Effects on Long Term Performance.

5a. CONTRACT NUMBER

5b. GRANT NUMBER
F49620-01-1-0079

5c. PROGRAM ELEMENT NUMBER

6. AUTHOR(S)
Gregory B. McKenna and Sindee L. Simon

5d. PROJECT NUMBER

5e. TASK NUMBER

5f. WORK UNIT NUMBER

7. PERFORMING ORGANIZATION NAME(S) AND ADDRESS(ES)
Department of Chemical
Engineering
Texas Tech University
Lubbock, TX 79409-3121

8. PERFORMING ORGANIZATION REPORT NUMBER
N/A

9. SPONSORING / MONITORING AGENCY NAME(S) AND ADDRESS(ES)
Air Force Office of
Scientific Research
AFOSR/NL
801 N. Randolph St., Ste 732
Arlington, VA 22203-1977

20040315 025

12. DISTRIBUTION / AVAILABILITY STATEMENT
Approve For Public release: Distribution unlimited.

13. SUPPLEMENTARY NOTES

14. ABSTRACT We extended a previous model due to the PIs for the evolution of the properties of curing thermoset resins to the BMI/SOC resins of interest to the Air Force. The model was used to estimate the cure stresses in this system in an ideally and isotropically constrained system. The results were surprising in the large magnitude of the stresses predicted and showed that judicious selection of polymer materials for low values of the thermal pressure coefficient will reduce thermal stresses by as much as a factor of three. Also, two distinct methods for measuring isotropic residual stresses were developed and demonstrated. A spherical "bomb" geometry was developed and provided a method of measuring isotropic stresses during cure when stresses remained below approximately 35 MPa. A thick-walled cylindrical geometry combined with lock-in amplifier electronics to excite the strain gages was developed for high stress measurements--pressures as high as 300 MPa were readily achieved, which is not possible with conventional thin-walled cylinders or with the thin-walled sphere just mentioned. More importantly, in the process of developing the thick-walled cylinder method, we demonstrated that the classical thin-walled tube method of constraining resins in an isotropic state of stress does not actually produce the isotropy expected. Measurements tend to be incorrect and are biased by the fact that the stresses are anisotropic. Hence, the thick-walled cylinder is a true improvement in measurement technology. Using this geometry, we performed the entire cure and post-cure under compression and observed over two hundred MPa cure stresses for model thermosetting resins—consistent with our model predictions. Our work leads us to conclude that reduction of isotropic residual stresses in thermosetting composites must focus on the reduction of thermal stresses through a reduction in the thermal pressure coefficient rather than focusing on reducing cure shrinkage.

15. SUBJECT TERMS
Ring opening polymerization, residual stresses, group contribution methods, cure shrinkage, thermosets, BMI resins, SOC resins, thermal stresses

16. SECURITY CLASSIFICATION OF:			17. LIMITATION OF ABSTRACT	18. NUMBER OF PAGES	19a. NAME OF RESPONSIBLE PERSON
a. REPORT	b. ABSTRACT	c. THIS PAGE		34	Gregory B. McKenna
					19b. TELEPHONE NUMBER (include area code) 806-742-3553

AFOSR Award No. F49620-01-1-0079
Report for Granting Period 12/1/00 to 11/30/03
Final Report

Project Title: Residual Stresses in Thermosetting Resins for Polymer Matrix Composites: Modeling and Effects on Long Term Performance

Investigator: Gregory B. McKenna
Co-PI: Sindee L. Simon
Affiliation: Department of Chemical Engineering, Texas Tech University

Summary

The present project had as its initial focus the modeling and measurement of residual stress development during cure and cooling of a bismaleimide resin copolymerized with a spiroorthocarbonate (BMI/SOC). The spiroorthocarbonate resin was incorporated because it undergoes a ring opening reaction and was anticipated to provide lower cure shrinkage and concomitantly lower cure induced residual stresses. Low residual stresses are important in many composite materials applications. During the course of the project we have developed modeling procedures and predictions for the isotropic residual stress build-up in the BMI/SOC resin and we have developed and analyzed two novel residual stress "bomb" methods of measuring the isotropic stress development during cure and subsequent curing of thermosetting resins. Both modeling and the development of the "bomb" method were highly successful during the course of the project. At the same time, the actual measurement of the residual stress development of the BMI/SOC copolymer was a continual problem. We have concluded that the problems we encountered were related to the volatility of the SOC monomer, whose vapor pressure is such that it volatilizes appreciably during mixing and completely at temperatures well below the cure temperature. This result is consistent with previously reported, but unexplained, extreme low densities obtained by other researchers for the SOC material. The results indicate that the BMI/SOC system that we have investigated is not viable for structural composite applications.

While the project was not fully successful due to the volatility of the chosen SOC material, we did make several significant contributions to the state of knowledge. First, we extended a previous model due to the PIs for the evolution of the properties of curing thermoset resins to the BMI/SOC resins. The prior model was for epoxy-type resins and this model generalized the other to the polymerization and copolymerization of the BMI/SOC system. In addition, the model was used to estimate the cure stresses in this system in an ideally and isotropically constrained system. The results of the study were surprising in the magnitude of the stresses predicted and also showed that judicious selection of polymer materials for low values of the thermal pressure coefficient offers the possibility of reducing thermal stresses by as much as a factor of three. In addition, during the course of the work, two distinct methods for measuring isotropic residual stresses were developed and demonstrated. First, we used a spherical "bomb" geometry which was successful in providing a method of measuring isotropic stresses during cure when stresses remained below approximately 35 MPa. This method was limited to the low stress regime due to the chosen thin walled spherical geometry, which gives isotropic stresses and high sensitivity of the measurement. However, thick-walled spherical vessels were not readily available and this lead us to develop a technique that uses a thick-walled cylindrical

geometry combined with lock-in amplifier electronics to excite the strain gages. The method was highly useful for two reasons. First, it overcomes the problems encountered in thin-walled systems because pressures as high as 300 MPa were readily achieved, which is not possible with conventional thin-walled cylinders or with the thin-walled sphere just mentioned. More importantly, in the process of developing the thick-walled cylinder method, we demonstrated that the classical thin-walled tube method of constraining resins in an isotropic state of stress does not actually produce the isotropy expected. Hence, the measurements tend to be incorrect and observations of failure within such tubes is biased by the fact that the stresses are anisotropic. Hence, the thick-walled cylinder is a true improvement in measurement technology. Using this geometry, we are able to perform the entire cure and post-cure under compression, and in doing so, we observed over several hundred MPa cure stresses for model thermosetting resins. In addition, we have shown that in open vessels, the magnitude of the tensile stresses that can build up during cure is significantly lower than expected and the value depends on the cure temperature with higher cure temperatures yielding lower stresses presumably due to increased microcavitation of the partially cured gel. This finding explains why fiber-reinforced thermosetting composites can be used successfully in spite of theoretical expectations of very large cure-induced tensile stresses. Our work leads us to conclude that reduction of isotropic residual stresses in thermosetting composites must focus on the reduction of thermal stresses through a reduction in the thermal pressure coefficient rather than focusing on reducing cure shrinkage.

Principal Findings

- Modeling studies of the isotropic stress build-up during cure and subsequent thermal history in a novel bismaleimide/spiro-orthocarbonate (BMI/SOC) thermosetting resin show that the SOC ring-opening reaction can reduce isothermal cure stresses by 17 % for optimum relative reaction rates of the BMI addition and SOC ring-opening reactions. A reduction of residual stress at room temperature of approximately 6% is predicted based on nominal values of the material parameters.
- A parametric analysis demonstrates that the reduction in isotropic residual stresses at room temperature is also dependent on the values of the thermal expansion coefficients and the bulk moduli in the glass and rubbery regimes (α_r, α_g, K_r, and K_g). The product $\alpha_r K_r$ (thermal pressure coefficient γ_r) influences the magnitude of the cure-induced residual stresses of the glass, whereas the product $\gamma_g=\alpha_g K_g$ influences the magnitude of the thermal stresses.
- Although isotropic stresses may only be reduced a few percent (depending on the relative magnitude of the cure and thermal stresses), this is predicted to provide significant lifetime improvement since lifetime is proportional to the stress raised to a very strong power.
- The first ever measurements of the product αK in both liquid and glassy states for thermosetting resins were made using a sealed stainless steel spherical pressure vessel which imposes an isotropic stress state on the material. The results indicate that $\alpha_g K_g$ is considerably smaller than $\alpha_r K_r$, an important finding for modeling residual stresses. This result differs from assumptions we made in our prior modeling, as well as assumptions

made by researchers at Sandia National Laboratories in their models of residual stress development in curing thermosets.

- Tensile cure stresses did not build up above a few MPa in our pressure vessels presumably due to gel fracture and/or debonding between the resin and the pressure vessel. This is a very significant result since this effect is not incorporated into any current models of residual stress build-up.
- The spiro-orthocarbonate comonomer was found to volatilize during mixing and during the temperature ramp to the cure temperature, indicating that its use in structural composite applications is not feasible.
- The stress distribution in the thick-walled tube was found to be isotropic. In addition, we found that the anisotropic distributions observed in thinner walled tubes is due to compliance of the tubes in the hoop direction. This finding explains why the conventional thin-walled tube geometry for measuring isotropic stresses does not give satisfactory results.
- The magnitude of the tensile stresses that build up in model epoxy resins cured in open vessels and, presumably, the degree of microfailure in the gel, depends on the cure temperature. This result is significant and is not incorporated into any current models of residual stress build-up.
- The coefficient of thermal pressure in the glass, $\gamma_g = \alpha_g K_g$, depends on the value of the first cure temperature in two step cures. For a model epoxy resin cured in an open vessel γ_g decreases as the cure temperature increases. Presumably this is due to the degree of microfailure that occurs in the curing resin. The result is significant because it shows, for the first time to the authors' knowledge, that the coefficient of thermal pressure in the glass depends on the cure history, and the result suggests that other properties may also depend on cure history.

Major Accomplishments

- Modeled the development of isotropic residual stresses in a novel SOC/BMI thermosetting material. The volume versus conversion and the T_g versus conversion relationships were estimated using the group contribution methods of van Krevelen and using statistical recursive theory.
- Performed a parametric analysis and determined the effect of various parameters on the isotropic residual stresses, including cure cycle parameters and material parameters.
- Developed an isotropic stress "bomb" method for measuring the thermal pressure coefficient $\gamma=\alpha K$ in the liquid and glassy states of thermosetting resins and made measurements for several thermosetting systems, including the novel BMI/SOC resin.
- Performed thermogravimetric measurements of the BMI/SOC resin system and established that the volatilization of the SOC component makes clear that this resin system is not applicable for structural composites.
- Completed the development of an instrument for measuring isotropic stress development in curing resins having a thick-walled tubular geometry using a lock-in amplifier

technique to measure strain. The method has advantages over the spherical pressure "bomb" geometry in that thermal pressures of over 300 MPa can be measured. In addition, the cure stresses can be quantified over the entire conversion range by keeping the resin in a compressive stress state throughout cure.

- Completed the calibrations, reproducibility studies, and test measurements on a fluid with known PVT properties for both the spherical and tubular isotropic stress instruments in order to demonstrate the range and accuracy of the measurements.
- Completed measurements and analyses of a model epoxy resin in both the tubular and spherical isotropic stress instruments. The model epoxy resin was used for measurements because its curing reactions do not change with cure temperature; hence, the effects of cure temperature independent of changes in cure chemistry can be evaluated.

Description of Work

Introduction

The work under the present project had multiple facets. First, because the goal was to evaluate the potential for the BMI/SOC resin system to reduce isotropic residual stresses induced during cure and subsequent cooling, we extended a model of resin property evolution and stress build-up during cure and cooling that had been developed by the PIs to the BMI/SOC system. This is described below. We then had to develop a method to measure the isotropic stress build-up and demonstrate how it worked. In the process we developed a spherical vessel or "bomb" method of measuring isotropic stress development in thermosets during cure and subsequent cooling. The method and results of measurements are presented below. An important outcome of this segment of the work is the finding that isotropic tensile curing stresses do not build up to the high levels anticipated from the modeling which indicates that cure shrinkage is not a major issue in the development of residual stresses in thermosets. The caveat here is that the mechanism that leads to the smaller-than-expected stresses is not completely understood and may cause changes in the final properties of the cured material. Because the spherical vessel method was limited to stresses below 35 MPa, we also developed a thick-walled tube method for measuring the isotropic stress development of thermosetting resins. This method overcomes both the limitations of the conventional thin-walled tube method and those of the thin-walled spherical vessel. The method permits measurements to internal stresses of over 300 MPa and shows the entire range of stress development during resin cure and cooling. The results support the findings in the thin-walled sphere that large negative (tensile) hydrostatic stresses cannot develop during thermoset cure even though the results also demonstrate that the stress changes due to cure shrinkage can be well over 150 MPa. The method can also be used to make fundamental measurements of the thermal pressure coefficient in liquids and glasses. Finally, the chemistry of thermosetting resin systems was investigated. We made the finding that the BMI/SOC resin designated for study in this work volatilizes during the mixing and curing process and this is discussed subsequently.

Modeling of the BMI/SOC Cure

The model used here to describe the development of isotropic residual stresses during cure of a novel BMI/SOC resin is based on an extension of our thermoviscoelastic model[1] We provide a brief description of the model and then focus our attention on the results of parametric studies.

The isotropic residual stresses, $\sigma_{res}(t)$, in a three-dimensionally constrained resin are given by the convolution integral:

$$\sigma_{res}(t) = -\int_{t_{gel}}^{t} K(t-t', T, x_1)\left(\frac{1}{V}\left[\frac{\partial V}{\partial x_1}\frac{dx_1}{dt'} + \frac{\partial V}{\partial x_2}\frac{dx_2}{dt'}\right] + \frac{1}{V}\frac{\partial V}{\partial T}\frac{dT}{dt'}\right)dt' \quad (1)$$

where K(t-t', T, T_g) is the bulk modulus, t-t' is the time elapsed from the time t' of the applied differential strain (due to cure shrinkage or temperature changes), $\left(\frac{\partial V}{\partial x_1}\right)_T$ and $\left(\frac{\partial V}{\partial x_2}\right)_T$ are the changes in volume per unit conversion of the BMI addition and SOC ring-opening reactions, respectively, dx_1/dt and dx_2/dt are the reaction rates of the two reactions and T is the absolute temperature. $\frac{\partial V}{\partial T}$ is the change in volume with respect to temperature and $\frac{dT}{dt}$ is the change in temperature in the cure cycle or any subsequent thermal history such as cooling.

The bulk modulus is assumed to depend on time, temperature and conversion in the following manner:

$$K(t, T, T_g) = K_r + (K_g - K_r)\sum_{i=1}^{n} g_i e^{\frac{-t}{a_{T,Tg}\tau_i}} \quad (2)$$

where K_r and K_g are the rubbery and glassy values of the bulk modulus, both of which are assumed to not be a strong function of temperature or conversion and t is time. τ_i is the i^{th} relaxation time at the reference temperature ($T_{ref} = T_{g\infty}$) and g_i is the weighting factor for the i^{th} relaxation time, such that Σg_i=1.0. The dependence of the relaxation time τ_i on temperature and conversion is accounted for by applying the principles of time-temperature[2,3] and time-T_g[4,5] superposition:

$$\log a_{T,Tg} = \frac{C}{T - T_\infty} - \frac{C}{T_g - T_\infty} \quad (3)$$

where C and T_∞ are constants.

To complete the model, the relationship between T_g and conversion is needed, as well as the cure kinetics. For the BMI/SOC system, the reactions are chain reactions with the result that the reaction mixture will be composed of monomer and high molecular weight polymer. Consequently, the glass temperature T_g is assumed to depend on the weight fraction of monomer and polymer, $w_{monomer}$ and $w_{polymer}$, respectively, through the Fox equation[6]:

$$\frac{1}{T_g} = \frac{w_{monomer}}{T_{go}} + \frac{w_{polymer}}{T_{g(polymer)}} \quad (4)$$

where T_{go} is the T_g of the monomer, $T_{g(polymer)}$ is the glass temperature of the cross-linked polymer which is a function of the cross-link density as predicted by DiMarzio[7] and modified by Hale, Macosko and Bair[8]:

$$T_{g(polymer)} = \frac{T_{gu}}{1 - \frac{KX}{1 - \psi X^2}} \quad (5)$$

where T_{gu} is the glass temperature of uncrosslinked polymer, K and ψ are constants and X is the crosslink density in the BMI/SOC network. Applying the recursive technique of Miller and

Macosko[9,10] to chain reactions, we can relate the weight fraction of monomer and polymer and the crosslink density X to the conversion x:

$$w_{\text{monomer}} = (1-x_1)^2 (2 - x_2)/2 \tag{6}$$

$$w_{\text{polymer}} = 1 - w_{\text{monomer}} \tag{7}$$

$$X = x_1^2 \tag{8}$$

In deriving equation 8, it was assumed that only the BMI addition network contributes to the crosslink density due to the flexibility of the SOC homonetwork.

The cure kinetics of the BMI/SOC system are assumed to be first order reactions:

$$\frac{dx_1}{dt} = k_1(1 - x_1) \tag{9}$$

$$\frac{dx_2}{dt} = k_2(1 - x_2) \tag{10}$$

where x_1 and x_2 are conversions of the BMI and SOC ring-opening reactions, respectively, and k_1 and k_2 are their respective rate constants.

Parameter Estimation

In order to evaluate the influence of the cure chemistry and resin properties on the development of isotropic residual stresses in the BMI/SOC resin, we need to estimate some particular parameters such as the relative volume changes involved in the ring-opening and addition reactions, the volume change due to the thermal history (i.e., the thermal expansion coefficient), the bulk moduli in the rubbery and glassy regions, and the dependence of the glass temperature T_g on the network formed (i.e., T_g versus conversion relationship).

The relative volume shrinkage per unit conversion for each reaction in the BMI/SOC system can be determined from the Van Krevelen group contribution method[11] which allows the molar volume of a monomer (or polymer) to be estimated as a function of its structure. This method assumes that molar volumes of the constituent groups are additive. For some constituent groups in the BMI/SOC resin, the molar volume contributions were not tabulated. We assumed for these groups that the molar volume contribution was equivalent to 1.5 times the van der Waals volume. The relative volume shrinkage for the BMI addition reaction is estimated to be -0.054 (-5.4%), whereas the relative volume expansion for the SOC reaction in the BMI/SOC network is found to be 0.009 (0.9%), both values are relative to the total volume of BMI/SOC polymer. The total relative volume change on full conversion of both reactions is -0.045 (-4.5%). Based on these estimates, at full conversion the SOC ring-opening reaction reduces cure shrinkage by 17%.

The nominal values of the thermal expansion coefficients in the glassy and liquid regimes, α_g and α_r, used in the majority of the modeling work are the average of data reported[12] for several polymers [polycarbonate, poly(methyl methacrylate), polystyrene, poly(vinyl acetate), polysulfone and poly(2,6-dimethylphenylene ether)]. The average values are $\alpha_g=2.55\times10^{-4}$ K^{-1} and $\alpha_r=6\times10^{-4}$ K^{-1}. In the same way, the nominal value of the bulk moduli in the glassy and rubbery regions, K_g and K_r, used in the majority of the modeling work were calculated from the average values reported for the same polymers. These values are $K_r=1.75\times10^9$ Pa and

$K_g=3.1\times10^9$ Pa. Since the values assumed for the thermal expansion coefficients and the bulk moduli will influence the magnitude of the isotropic residual stresses, we also performed a parametric analysis of these effects.

The dependence of the glass temperature on the conversion is needed for the model and, as shown in equations 4 and 5, the relationship depends on the values of the glass transition of monomer, that of the uncrosslinked polymer T_{gu}, as well as on the constants K and ψ. The glass transition temperature of the monomer (T_{g0}) for the BMI/SOC system is determined from the values of the glass temperature of BMI and SOC monomers using the Fox equation and assuming that the T_g of the monomers is related to their melting temperature by $(T_{g0i}/T_{mi})=0.75$. The melting temperature T_m of the Ciba Geigy Matrimid 5292A (BMI) and the spiro-orthocarbonate (SOC) monomers are 425.56 K and 303 K, respectively.[13] The value T_{go} of the BMI/SOC monomer is estimated to be 265 K. The glass transition temperature of the uncrosslinked polymer, T_{gu}, was calculated using the Van Krevelen's group contribution method[11] and was found to be 392 K. The parameters K and ψ in equation 5 were found by fitting the experimental data of Morgan et al.[14] of a model of BMI Matrimid part A and part B resin cured at 250°C. The values of K and ψ were calculated to be 0.218 and 0.1, respectively. By applying equation 5 and using these values, the value of $T_{g\infty}$ of the BMI/SOC resin at full conversion is estimated to be 244°C.

Evaluation of the effect of the ring-opening reaction on isotropic residual stresses

We calculated the cure-induced isotropic residual stresses for the BMI/SOC resin by first assuming that the addition and ring-opening reactions have identical rates. Figure 1 shows the evolution of isotropic residual stresses during isothermal cure and subsequent cooling for two cases, one in which ring-opening occurs and the other in which it does not. The simulations were performed for an isothermal cure at T_c=250°C for approximately 60 min followed by cooling to room temperature at 10°C/min. In this simulation, $k_1=k_2=0.0025$ (s^{-1}). Figure 1 shows that the isotropic residual stresses begin to increase immediately at zero time because gelation occurs as soon as the BMI addition reaction begins. The stresses level off as full conversion is reached. Upon cooling (which begins at approximately 60 min) the hydrostatic residual stresses again increase. It can be seen in Figure 1 that the stresses that arise due to shrinkage during cure are significant and that the ring-opening reaction decreases the cure stresses by 18.5 MPa or about 17% at T_c. This reduction of 17% is obtained when the addition and ring-opening reactions have identical rates and assuming that T_g is unaffected by the ring-opening reaction. Larger or smaller reductions may be expected if the reactions are sequenced differently. The thermal stresses are unaffected by the ring-opening reaction since they depend on $\alpha_r K_r(T_c\text{-}RT)$. Hence, at room temperature the residual stresses are still 21.3 MPa lower when ring-opening occurs,

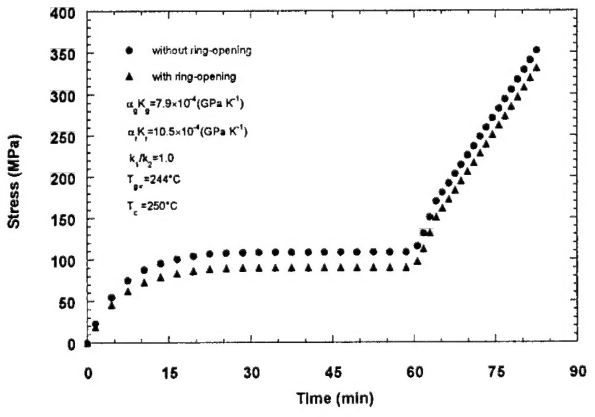

Figure 1: Evolution of isotropic residual stresses during cure at 250°C and subsequent cooling to room temperature as a function of time of cure for the BMI/SOC and BMI resins for $k_1=k_2=0.0025(s^{-1})$.

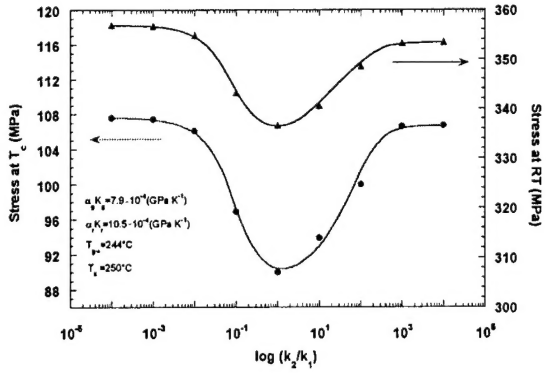

Figure 2. Isotropic residual stresses after 60 min. cure the cure temperature and at room temperature as a function of the relative reaction rate ratio k_2/k_1 with k_1=0.0025 s^{-1}.

but this is now only a 6% decrease of the total residual stress relative to the case where ring-opening does not occur.

In order to show how the isotropic residual stresses during cure depend on the sequencing of the addition and ring-opening reactions in the BMI/SOC resin, we varied the relative rate ratio. Figure 2 shows the effect of the relative reaction rate ratio on the isotropic residual stresses in the BMI/SOC system for a one-step cure held for 60 minutes at 250 °C. The stresses are shown both at the cure temperature and after at cooling to room temperature. The isotropic residual stresses at the cure temperature are always less than the stresses at room temperature, but for the parameters chosen for these calculations, the residual stresses due to the cure shrinkage (i.e. those at T_c) may contribute from 25 to 30% of the total stresses. The shape of the curve in Figure 2 is related to the extent of the the ring-opening reaction that occurred after gelation. There is a minimum in the cure at intermediate values of k_2/k_1. If the ring opening reaction is too slow and does not occur in the time scale of the isothermal cure (very low k_2/k_1) no expansion will occur after gelation and the isotropic residual stresses will be high. At intermediate k_2/k_1, there is a regime where the ring opening reaction occurs on a time scale comparable to or slightly slower than that of the addition reaction-fast enough to achieve significant cure in the time scale of the isothermal cure, but slow enough that much of the ring opening occurs after gelation of the system. On the other hand, if the ring opening reaction is too fast and expansion occurs prior to gelation of the system (very high k_2/k_1), again the isotropic residual stresses will be high.

Evaluation of the effect of the cure histories on isotropic residual stresses

The results of one-step cure and ramp/hold cure cycle simulations are summarized as a function of the cure temperature at which gelation occurs (T_{gel}) in Figure 3. A linear relationship between residual stress and T_{gel} is obtained for both one-step and ramp cures if vitrification does not occur during cure, i.e., if during the cure the bulk modulus can relax to its rubbery value. These results demonstrate that the cure temperature at which gelation occurs is an important parameter for optimizing cure histories in efforts to lower isotropic residual stresses. However, lowering the temperature at which gelation occurs results in longer, slower cure cycles and, therefore, an increase in the cost of manufacturing.

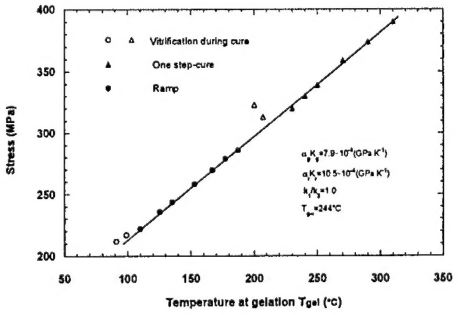

Figure 3. Isotropic residual stresses at the end of cure at room temperature for one step isothermal and ramp/hold cure histories as a function of the cure temperature at which the material gelled (T_{gel}). The filled and unfilled symbols indicate cure histories where vitrification did not or did occur during cure, respectively. The line represents the relationship obtained in the absence of vitrification. ($k_1=k_2$=0.0025 s^{-1}).

Evaluation of the effect of material parameters

Figures 4 and 5 show the effects of varying the product $\alpha_g K_g$ and $\alpha_r K_r$, respectively, on the magnitude of the isotropic residual stresses in the fully-cured material at room temperature for one-step cure cycles. The value of $\alpha_g K_g$ influences the magnitude of thermal stresses and decreasing the value significantly reduces the isotropic stresses at room temperature. On the other hand, the value of $\alpha_r K_r$ influences primarily the magnitude of the shrinkage-induced cure stresses. In this case, decreasing the product of the expansion coefficient times the bulk modulus reduces stresses both at the cure temperature and at room temperature.

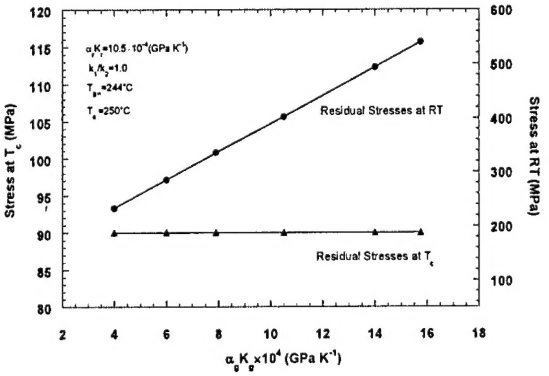

Figure 4: The effect of the product $\alpha_g K_g$ on the isotropic residual stresses at T_c and room temperature (RT) for cure at 250°C for one hour followed by cooling at 10°C/min to RT.

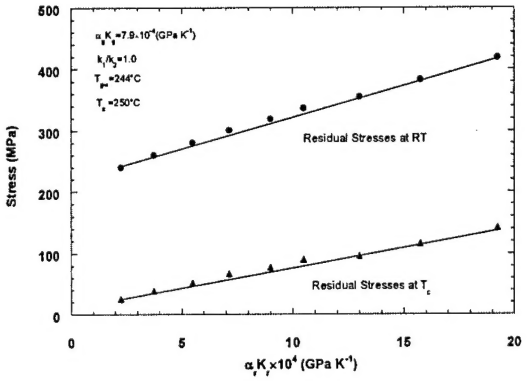

Figure 5: The effect of the product $\alpha_r K_r$ on the isotropic residual stresses at T_c and room temperature (RT) for cure at 250°C for one hour followed by cooling at 10°C/min to RT.

Implications

Reducing residual curing stresses in the BMI/SOC copolymer are expected to enhance mechanical properties and improve the long term performance of the polymer matrix composite. Moreover, reducing isotropic residual stresses after cure at room temperature by about 6% should increase the time to failure of the material. McKenna and Penn[15,16] and Crissman and McKenna[17] found that the time-dependent failures of several polymers and rubbers could be characterized within the framework of a cumulative damage model for failure. In those studies, the mean failure times in constant rate of stress experiments were successfully predicted from a model using a time to fail function determined from constant stress experiment (i.e., the time to fail is described by an exponential function of the applied stress). According to that body of work, decreasing applied stresses by 6% should increase the time to failure by approximately a factor of 4 (e.g., $t_{fail} = t_{fo}\,\sigma^{-19.4}$ for PMMA). A similar analysis of fatigue lifetime of an epoxy resin[18] yields an exponent of -13 such that the time to failure would increase by 2.2 for a 6% reduction in residual stress.

Conclusions from modeling

A thermo-viscoelastic model of isotropic residual stress development in thermosets was extended to a novel BMI/SOC thermosetting resin system. The influence of the cure chemistry and resin properties on the build-up of isotropic residual stresses has been evaluated. The results show for the case where the addition and ring-opening reactions have identical rates that the

isotropic residual stresses during cure and after cure at room temperature are reduced by 17% and 6%, respectively. The optimal sequencing of addition and ring-opening reactions in the BMI/SOC system is such that the ring-opening reaction is slow enough so that it occurs only after gelation of the system, yet is fast enough to achieve full conversion in a reasonable time frame.

In addition, we have examined the influence of cure cycle and material parameters. Isotropic residual stresses can also be reduced by gelling at lower temperatures and by reducing the product of the thermal expansion coefficient times the bulk modulus. This latter observation suggests new strategies may be developed beyond the current ring-opening chemistries that could also enhance composite material performance.

Experimental Methods

Materials

The material of primary interest in this study was designated by the Air Force as the novel BMI/SOC system, containing Matrimid 5292A, Matrimid 5292 B (both from Ciba Geigy Corp.) and a spiro-orthocarbonate comonomer (Polycomp Technologies) mixed in a 1.0:0.75:0.25 molar ratio. The 5292A is cured by the allyl groups on both the 5292B resin and the SOC comonomer. In addition, the SOC can undergo a ring-opening reaction catalyzed by triphenylsulfonium hexafluorophosphate. We studied both a system in which the catalyst was added at 5 weight percent of the SOC and a system in which catalyst was not added. For both systems, we heated Matrimid 5292 B component and the SOC comonomer together at 140 °C and then mixed in the Matrimid 5292 A until the mixture was homogeneous (15 to 20 minutes). For the catalyzed system, the solid catalyst was weighed out separately on the scale and DMF (dimethyl formamide) was added dropwise and mixed until the catalyst dissolved. The weight percentage of DMF used was 3 to 4% of the total mass of the system. The catalyst solution was added dropwise to the A/B/SOC mixture while the mixture was stirred and then mixed an additional 10 minutes. Due to concerns about the effects of any residual DMF left in the system after mixing and degassing, a solvent-free mixing process has been developed. In this case, the catalyst was dissolved into the Matrimid 5292B component at 160 °C for 15 to 20 minutes. Then the Matrimid 5292A and SOC were added after the mixture had cooled to between 130 and 140 °C and mixed for 15 to 25 minutes until the mixture was homogeneous. All results reported here for the catalyzed system are for the system mixed using solvent.

In addition to the BMI/SOC system, two model thermosetting systems were also examined. A model BMI system consisted of Matrimid 5292A cured with Matrimid 5292B in a 1:1 stoichiometric ratio with mixing accomplished at 140 °C for 15 to 20 minutes until the system became homogeneous. A model bifunctional epoxy (diglycidyl ether of bisphenol A, DGEBA; DER 332, Dow Plastics) cured with a tetra-functional aromatic amine (trimethylene glycol-di-p-aminobenzoate, TMAB; Versalink 740 M, Air Products) in a 1:1 stoichiometric ratio was also studied. The epoxy was mixed following a procedure described by Simon and Gillham [1].

All BMI resin solutions were degassed after mixing at 130 °C for 15 minutes and the epoxy mixture was degassed at room temperature. The solutions were stored in the freezer in sealed vials placed in a larger container with desiccant until use.

Residual Stress Measurements

Two methods are compared for measuring isotropic residual stresses during cure and subsequent thermal history. We first present the novel method developed in this project of using

an instrumented spherical bomb to contain the resin during cure and subsequent cooling to provide isotropic stresses. The second method is that of a thick-walled tube method which we subsequently developed to overcome the shortcomings of the thin-walled sphere method; in addition, the thick-walled tube overcomes the shortcomings of the conventional thin-walled tube method. In both tube methods, the tube is long relative to the inside diameter. In principle, isotropic stresses are developed in the inner portion of the tube away from the ends. We show that this method does not result in isotropic stresses in the thin-walled tube geometry–something that has been reported previously in the literature[19-21], but not fully explored. We show that the thick-walled tube can be successfully used to create isotropic constraints on the solidified polymer and that we can measure them in spite of the small deformations in the thick walls because of the use of lock-in amplifier electronics which are up to 20 times more sensitive than those used in conventional strain-gage work.

Design of the Instrumented Sphere

Figure 6 shows a schematic of the instrumented sphere for measuring isotropic cure and thermal stresses. Strain gauges are used to measure deformations in the outer wall of the sphere, enabling the pressure of the constrained material within the sphere to be calculated. In addition, thermocouples are used to measure thermal events. To minimize self-heating of the gauges on the relatively small vessel we used a low excitation voltage across the bridge. Use of a lock-in amplifier to measure bridge voltage instead of the common DC strain gauge amplifier method provides much better signal-to-noise ratio at the low excitation levels.

The stainless steel spherical pressure vessel (Fauske & Associates, Inc.), itself, is shown in Figure 7a. The size of the spherical vessel is 0.5 in. (12.7 mm) inner diameter, 0.02 in. (0.51 mm) wall thickness and 1/8 in. (3.18 mm) stem diameter. The stem length is 1 in. (25.4 mm). A separate vessel is used for each experiment. The strain at the outer surface of the vessels is

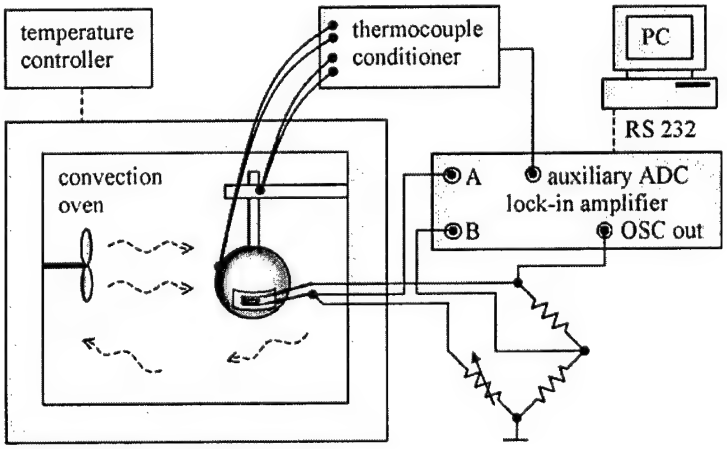

Figure 6. Schematic view of the instrumented sphere system for measuring isotropic residual stresses.

monitored by foil strain gauges, bonded to the vessel wall usually on the pole opposite the filling stem, as shown in Figure 7b. For minimum zero drift of strain readings at high temperatures we used FSM-Series gauges (BLH Electronics, Inc.) with nickel-chrome alloy for the sensing element (grid) and polyimide-glass for the carrier material (foil). Both 350 Ω and 120 Ω gauges were used during the present study. The gauges were bonded with a high-temperature adhesive

(PLD-700, BLH Electronics, Inc.). The adhesive was cured at 260°C for two hours and was postcured at 350°C for another two hours to minimize possible creep/drift of the gauges at working temperatures (up to 300°C). The gauges were wired in a Wheatstone bridge, which was connected to a lock-in amplifier (DSP-7265, PerkinElmer Instruments). The resistors completing the bridge were Vishay S102 type with a resistance temperature coefficient of 2 ppm/K. The balancing of the bridge was found to be unnecessary, since the offset output voltage for all gauges used fell well into the input range of the lock-in amplifier and this offset was canceled out after temperature compensation (see calibration section). The bridge excitation was driven by the lock-in oscillator at 100 Hz with a 1 V_{rms} programmed amplitude (actual amplitude was smaller because of the 50 Ω output impedance of the oscillator). The output of the bridge was connected to the differential input of the lock-in, operating in the first harmonic mode with a time constant of 100 ms. The noise level in the input voltage was of the order of 0.1 μV. Conventional strain gauge amplifiers, like the High Performance Strain Gauge Amplifier DMD-520, Omega Technologies, have a 5 μV input referred noise level specification. This would allow a strain resolution of about 8 μstrain at the 1.25 V excitation of the bridge using a single gauge circuit with a gauge factor of 2. The lock-in technique allows us to achieve 0.2 μstrain resolution at 1 V excitation. Additional limitations in strain readings are the degradation of the gauge with time and temperature fluctuations, which complicate the temperature compensation discussed in the calibration section. In order to check the isotropy of the stresses, tests were also run with two gauges bonded to different places on the vessel wall, at approximately 45° and -135° from the stem. We note that stainless steel vessels were chosen for the present study, although titanium and aluminum spheres were available. The reasons for this choice were 1) the steel vessel is stiffer than either the Ti or Al and 2) the Al would creep at the highest test temperatures of interest, i.e. 300°C.

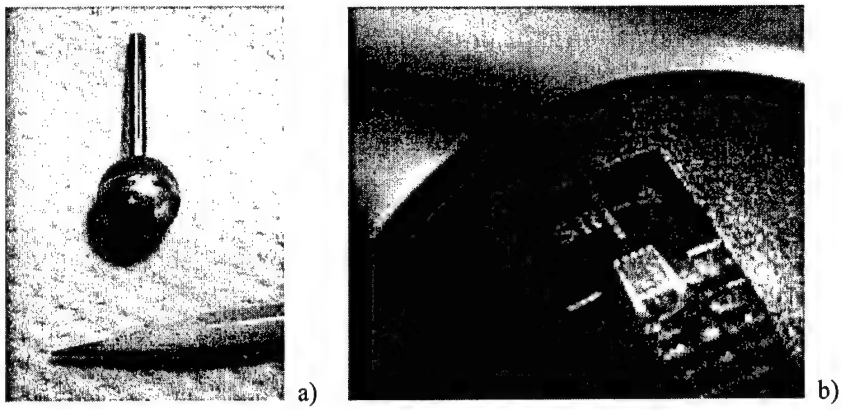

Figure 7. a) Stainless steel spherical pressure vessel with filling stem. b) Strain gauge bonded to the vessel surface.

The heat released due to an exothermic reaction inside the vessel results in a temperature gradient between the vessel and the oven. This gradient was measured using a thermocouple, type K, with the hot junction attached to the surface of the vessel and the cold junction attached to the vessel holder. The thermocouple signal after amplification to 10 mV/K was fed to the auxiliary ADC of the lock-in amplifier. Temperature and the strain gauge readings were recorded into an MS Excel spreadsheet via RS-232 interface using MS Visual Basic macros.

To obtain good thermal coupling between the vessel and the oven, we exposed the vessel to airflow in a fan assisted convection oven (Carbolite LHT4/30). The vessel followed the temperature-time program closely with a maximum temperature overshoot of 2 K due to the reaction exotherm. Shielding of the vessel from the airflow improves the resolution of the heat flow measurements by a factor of 7 to 10, but results in a very poor thermal coupling with slower response to the program temperature and larger temperature overshoots during cure. Thermal coupling could also be improved by immersing the pressure vessel into oil, but this affects the stability of the strain gauge, which is placed on the outer surface of the vessel.

The small size of the vessel was found to be very important for good thermal coupling between the curing resin and the surroundings. Experiments with larger spheres of 1 in. (25.4 mm) diameter showed "run-away" conditions during the cure reaction and a temperature overshoot of more than 40 K above the programmed temperature was measured when the sphere was in the convection oven. Decreasing the sphere diameter by a factor of two to 0.5 in. (12.7 mm) resulted in a 2 K overshoot under the same conditions. Spheres smaller than 0.5 in. (12.7 mm) in diameter are difficult to manufacture with isotropic properties since the relative size of the welding joints is large. In addition, the high surface curvature of smaller spheres would make it difficult to attach strain gauges.

Calibration of the Instrumented Sphere

To calibrate the internal pressure response in the instrumented sphere, the pressure vessel was connected to a hydraulic pressure generator and pressurized up to 30 MPa with a pressure-transmitting oil. The pressure generator was instrumented by a pressure gauge (Sensotec TJE/H126-01TJG) with 0.1% accuracy. After each pressure change the adiabatic temperature variations were allowed to equilibrate for 3 min, and the pressure gauge and strain gauge readings were recorded. The results of one measurement made at room temperature are shown in Fig. 8. The calibration factor is determined as the slope of the output-voltage/pressure curve with uncertainties below 0.5%. Since during the first pressurization some "fresh" vessels showed a small hysteresis on increasing and decreasing pressure, which disappeared in subsequent pressurization cycles, several pressurizations were performed and the calibration factor was determined from the data for the last pressurization. The pressure calibration agrees well with calculations of the calibration factor based on the vessel geometry. Since the oil pressure generator could not go to high temperatures, e.g., 250 °C, an additional calibration of the vessel was performed at 1MPa

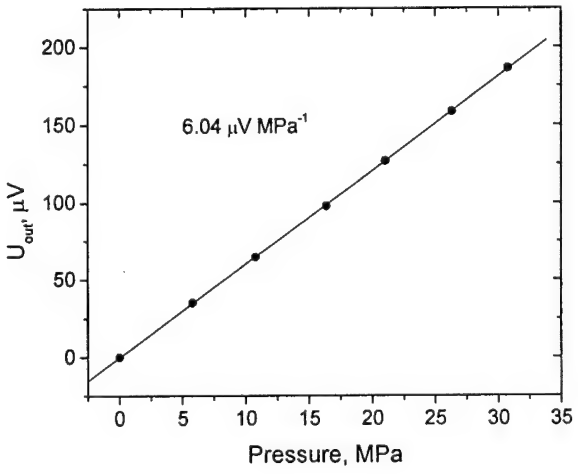

Figure 8. Output voltage changes due to pressurization the vessel at room temperature with pressure transmitting oil. Data points are shown with linear regression line and The resulting value for the slope.

using N_2 gas at room temperature and at 250°C in the oven. Within experimental uncertainty the calibration factor so determined was the same as that determined at room temperature with the oil pressurization.

The strain gauges are self-temperature compensated to balance the strain-generated resistance changes produced by the difference in thermal expansion coefficient α between the sensing element and the vessel. The vessels were made from SS-304 stainless steel. We found that in our system the minimum response to temperature change was shown by gauges with

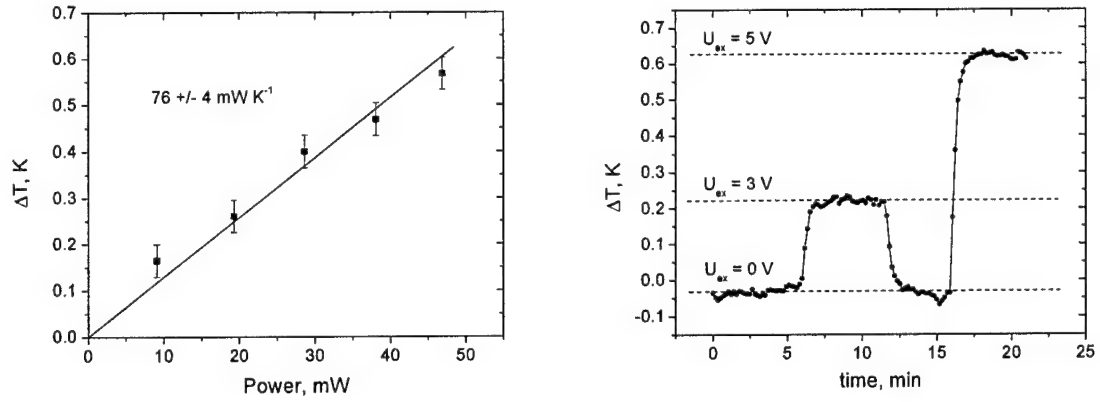

Figure 9. a) Temperature difference between the vessel and the oven, ΔT, vs time for various values of the excitation voltage, U_{ex}, at the bridge (programmed values are shown). b) ΔT vs the total power, released from two gauges. The value for the heat flow calibration factor is shown. The oven temperature is 140°C.

temperature compensation for mild steel ($\alpha = 1.08\times10^{-5}$/K), type S6, rather than for stainless steel ($\alpha = 1.62\times10^{-5}$/K), type S9.[22] The reason for this may be the elevated temperatures used in our work, since the self-temperature compensation is optimized near ambient temperature. In addition, the grid of the gauges is slightly deformed by the convex surface of the vessel and this may affect the self-temperature compensation. The remaining temperature compensation was accomplished by measuring a signal in the empty pressure vessel as a function of temperature and subtracting this function from the signals obtained for the same vessel filled with the material of interest. Following this procedure the resolution of temperature-induced stresses was on the order of 2 kPa/K.

The heat flow calibration for the instrumented sphere was performed by varying the excitation voltage applied to the bridge and measuring the temperature difference between the vessel and the oven. Due to Joule heating, the gauge released a known amount of power, which depended on the applied voltage. An example of the calibration is shown in Figure 9. The heat flow calibration factor is affected by the specific position of the vessel in the oven and can be determined for each vessel individually.

Design of the Instrumented Thick-Walled Tube

We used stainless steel thick-walled tubes of 0.25 in. (6.35 mm) outer diameter and 2.75 in. (70 mm) length (stainless steel nipple, High Pressure Equipment Co.) shown in Figure 10 as a means to impose 3D constraints on the material. The inner diameter was increased by boring through the cylinder length with a 7/64 in. (2.78 mm) drill bit. The same drill bit was used later to remove cured resin from the tube, making the tube reusable without the need to recalibrate. To

seal the tube we used standard closing fixture (caps, collars and glands, High Pressure Equipment Co.). In some experiments, the tube was intentionally left open at one end with the funnel used to fill the vessel with the liquid attached, in order to maintain a fully filled tube.

Figures 10 and 11 show the instrumented thick-walled tube and instrumentation. The foil strain gages are used to measure the tube deformations, from which the internal pressure of the constrained material can be calculated. The strain gages were bonded at the outer surface of the tube in hoop and in axial directions. The same strain gages, adhesive, and lock-in amplifier methodology was used as in the instrumented sphere method. However, a 0.5 V_{rms} programmed amplitude was used for bridge excitation in the case of the thick-walled tube, and the output of

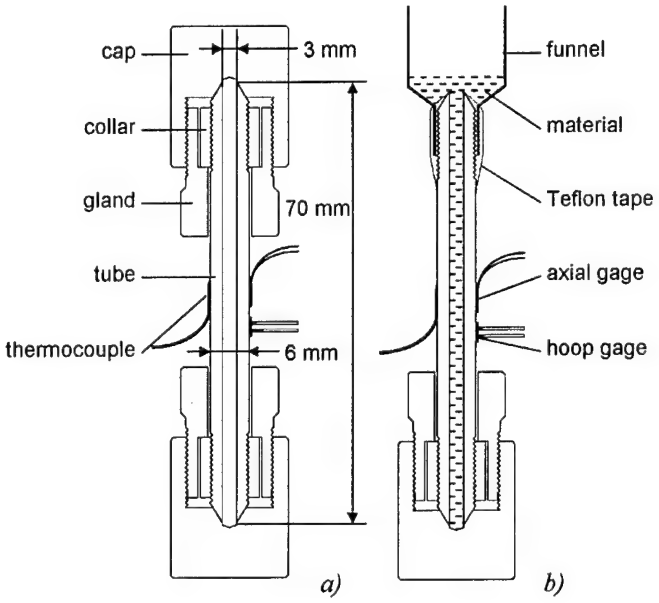

Figure 10. a) Cross-section view of stainless steel thick-walled tube pressure vessel with closing caps. b) Cross-section view of open vessel with a funnel.

the bridge was connected to the differential input of the lock-in amplifier, operating in the first harmonic mode with a time constant of 0.5 s rather than 0.1 s. In addition, a mechanical relay, operated by the auxiliary DAC of the lock-in amplifier, was used to switch automatically between hoop and axial gages output every 5 s. Data points were sampled with the same rate (one point every 5 seconds).

Use of a lock-in amplifier to measure bridge voltage instead of the common DC strain gage amplifier method provides much better signal-to-noise ratio at the low excitation levels and is necessary for measuring the strain in the thick-walled tube. The noise level in the input voltage was of the order of 50 nV. Conventional strain gage amplifiers, such as High Performance Strain Gage Amplifier DMD-520, Omega Technologies, have a 5 μV input referred noise level specification (in practice, the measured noise level is higher because of the noise in the source signal) allowing a strain resolution of about 8 μstrain at the 1.25 V excitation of the bridge using a single gage circuit with a gage factor of 2. The lock-in technique allows us to achieve

0.2 μstrain resolution at 0.5 V excitation. Increasing the excitation voltage in our case does not improve strain resolution due to self-heating of the bridge resistors, which leads to additional temperature drift, and therefore, additional resistance drift affecting signal stability. Other limitations on the strain resolution are the degradation of the gage with time and the temperature fluctuations of the tube, which complicate the temperature compensation. Since the compliance of the tube is very small, the strain readings, especially in the axial direction, are very sensitive to the temperature; i.e., the tube acts more like a thermometer, than a pressure gage. To alleviate this situation, careful temperature compensation is performed before any stress analysis by measuring a signal in the empty tube as a function of tube temperature and subtracting this function from the signals obtained for the same tube filled with the material of interest. Following this procedure the errors of temperature-induced stresses were on the order of 5 kPa/K and 20 kPa/K for hoop and axial stresses, respectively.

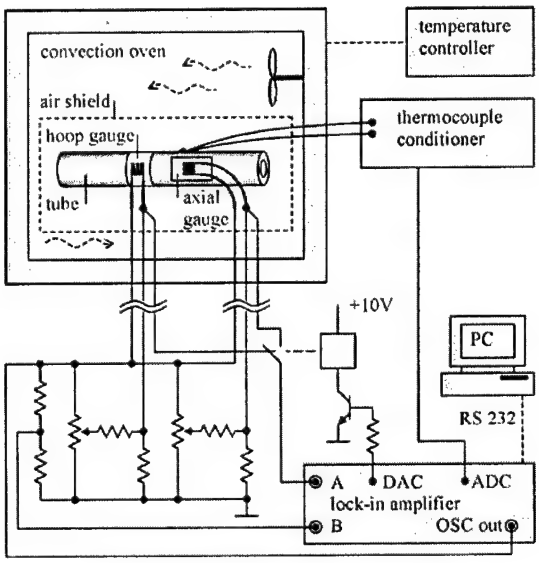

Figure 11. Schematic view of the instrumented thick-walled tube method.

The strain-gaged tube was placed in a fan assisted convection oven, Carbolite LHT4/30. To minimize the temperature gradient across the tube the latter was shielded from the airflow and heating and cooling rates were limited to 1 K/min. The temperature of the tube was monitored with a thermocouple, bonded to the outer surface of the tube in a similar way as the strain gages were bonded for better thermal contact. The thermocouple signal after amplification to 10 mV/K was fed to the auxiliary ADC of the lock-in amplifier. An additional thermocouple was attached to the bridge circuit. The temperature of the bridge stays within ±0.2 K over the course of several hours with a maximum swing of ±1.5 K from day to night. The ±1.5 K temperature variation leads to a maximum of ±3 ppm resistance changes in the bridge, resulting in approximately ±0.7 MPa and ±3 MPa maximum long-term instability in strain gage readings in hoop and axial directions, respectively (see Appendix for relevant equations). Temperature and strain gage readings were recorded by a computer into MS Excel spreadsheet via an RS-232 interface between lock-in amplifier and PC using MS Visual Basic macros. An experiment consisted of recording the strain gages readings and the actual temperature of the tube during the temperature-time program of interest.

Calibration of the Instrumented Tube

To calibrate the internal pressure response of the instrumented tube, the tubular pressure vessel was connected to a hydraulic pressure generator and pressurized to 330 MPa with pressure-transmitting oil. The pressure generator was instrumented by a pressure gage, Sensotec TJE/H126-01TJG, with 0.1% accuracy. After each pressure change the adiabatic temperature variations were allowed to equilibrate for 3 min, and the pressure gage and strain gage readings were recorded together with the tube temperature. The latter was used for further temperature compensation. The results of one measurement are shown in Figure 12a. The calibration factor is determined as the slope of the output-voltage/pressure curve with uncertainties below 0.3%. No hysteresis was observed on "fresh" tubes upon increasing and decreasing pressure. The pressure calibration agrees well with calculations of the calibration factor based on the tube geometry. Figure 12b shows that the calibrations are highly linear based on the residual voltages minus the linear fits.

a) b)

Figure 12. a) Output voltage changes due to pressurization of the tube with pressure transmitting oil. Data points are shown with linear fits and the values for the slopes for hoop and axial directions. b) Residual showing linearity of calibrations.

Thermogravimetric Experiments

Thermogravimetric analysis (TGA) was performed on the BMI/SOC resin using the TGA7 from Perkin Elmer in order to determine if resin volatility was the cause of lack of reproducibility, the unexplained very low thermal pressure coefficients, and the lack of SOC signature in the FTIR cure data. Experiments were performed under flowing nitrogen. Uncured resin samples were loaded at room temperature. A ramp was performed at 5 K/min to 140 °C which was the mixing temperature for the resin. After a hold of 30 minutes at 140 °C to simulate mixing, the material was ramped to 300 °C to simulate the ramp to the cure temperature.

Results

The Spherical Pressure Vessel: Calibration and Test Results

Calibration of Spherical Pressure Vessel

One of the reasons for developing the current experimental techniques was to ensure an isotropic stress state in the resin. We examined the stress isotropy in the spherical vessel by attaching two strain gauges below and above the welding joint of the vessel. We chose a low molecular weight glass former, sucrose benzoate, Aldrich Chemical Co., to test the isotropy of stresses in a solid (vitrified) state. The material was filled into the vessel at 150°C following the same procedure described previously with the difference that more time was allowed for the air

to leave the vessel (about an hour). After filling, the vessel was left opened. Figure 13 shows the development of tensile stresses inside the vessel measured by the two gauges during cooling from the liquid to the vitrified state. At high temperatures the material is a liquid and thermal shrinkage is compensated by material flow – there are no stresses in the vessel. The small increase in tensile stresses on cooling from 90°C to 70°C can be attributed to the high viscosity of sucrose benzoate at those temperatures – the material acts partly as a plug in the filling stem. The material vitrified at approximately 65°C, where it ceases to flow and further thermal shrinkage results in the development of tensile stresses until failure occurs at 47°C. The failure relieves most of the stresses. Before failure the stress versus temperature curves from the upper and lower gauges are almost identical, indicating good isotropy of the stress state. The 8% difference in stress between the two channels can be attributed to slight differences in local compliance of the vessel. The lower gauge in that measurement probed 13.44 μstrain/MPa whereas the upper gauge probed 12.05 μstrain/MPa. On thermal shrinkage the solid tries to impose the same strain in all directions, resulting in lower stress readings in the lower gauge in this particular case.

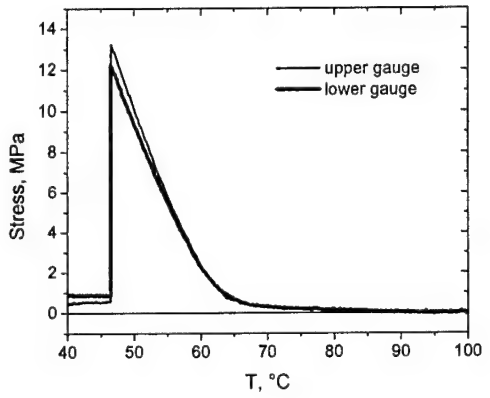

Figure 13. Hydrostatic stresses vs temperature in the spherical pressure vessel filled with sucrose benzoate during cooling at 1 K/min. The two stress curves correspond to stresses at the upper and lower parts of the vessel. The vessel was open during the measurement; hence stresses develop only upon vitrification of the sucrose benzoate.

Thermal Pressure of a Known Fluid in the Spherical Pressure Vessel

The thermal pressure of a known oil, confined in the spherical pressure vessel, was measured to check the accuracy of the calibration and the range of measured stresses. Di-2-ethylhexyl sebacate (MONOPLEX® DOS, C.P. Hall Company) was used because its PVT behavior is documented.[23] The oil was initially degassed for 20 hours in vacuum at room temperature. The strain-gauged vessel was then immersed into the oil container; oil did not flow into the vessel due to the small neck diameter. Then a vacuum was applied for 15 minutes to remove the air from the vessel. The vessel was then exposed to atmospheric pressure and the oil went into the vessel. Finally vacuum was applied once again to assure no gas was trapped in the vessel. After filling, the vessel was sealed using a threaded end cap (Swagelok Company) to close the open end. The development of thermally induced stresses in the oil during heating at 0.5 K/min is shown in Figure 14 for two strain gauges attached below and above the welding joint of the spherical pressure vessel. At the very beginning of heating the compressive stresses do not build up until the expanding oil occupies the cavity in the sealing cap at approximately 27°C. When the compressive stress in the vessel exceeds 30 MPa (at about 55°C), yield of the vessel wall

occurs (mainly along the weld joints), increasing the inner volume of the vessel and partly relieving the stress. Note that the relatively low yield point in the spherical pressure vessels is what led us to develop the thick-walled tube instrument which be used to over 300 MPa.

The apparent thermal pressure coefficient γ_{app}, which we measure as the slope in the stress-temperature curve, depends on the thermal expansion of the stainless steel (α_v) and on the

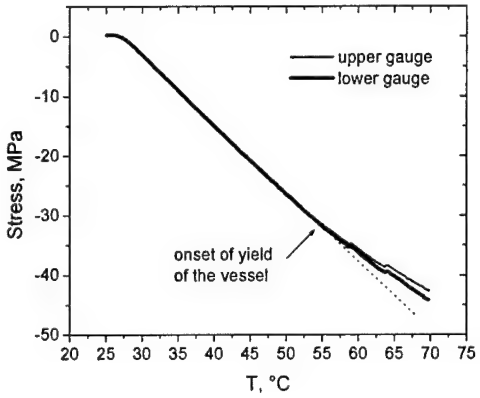

Figure 14. Thermally-induced compressive stress in a closed spherical pressure vessel filled with pressure transmitting oil as a function of temperature during heating at 0.5 K/min.

structural stiffness of the vessel (K_v): $\gamma_{app} = (\alpha - \alpha_v)\frac{K}{1 + K/K_v}$, where α is the coefficient of thermal expansion, K is the bulk modulus of the material (oil) . The measured γ_{app} was determined by fitting both stress/temperature curves in Figure 14 to a second order polynomial in the temperature range from 30°C to 55°C and taking the temperature derivatives of those fit. The average of two γ_{app} determinations from the two curves is shown in Figure 15 along with corrected and expected values, the latter of which are based upon PVT data from Sane and Knauss[23] calculated for the same temperature-pressure profile as the experiment shown in Figure 9. Our measurements after correcting for the thermal expansion and compliance of the vessel are approximately 4 % higher than expected based on the data of Sane and Knauss[23]. The discrepancy may be due to the values of the vessel parameters used for the correction; the vessel probably has lower coefficient of thermal expansion than we assumed (since the gauges with lower self-temperature compensation work better, as mentioned earlier) and also may have a higher value for structural stiffness K_v than estimated (since welding joints can act as a reinforcement and about 10% of the vessel volume is a much stiffer filling stem).

In a similar way we have also measured the thermal pressure of n-hexadecane (99%, Alfa Aesar). The measured value of γ is 10% to 15% above the expected value when corrected with the thermal expansion of the stainless steel $\alpha_v = 1.62\times10^{-5}$/K and structural stiffness of the vessel K_v = 16 GPa estimated from the geometry. The expected γ for hexadecane itself varies by 5% depending on details of the analysis of available PVT data (the material function of hexadecane is more complicated than that of the oil, because of the proximity to the crystal-melt transition). In addition, the γ estimated from the PVT data of Zoller and Walsh[24] is 11% to 14% higher than the γ measured by Orwoll and Flory.[25]

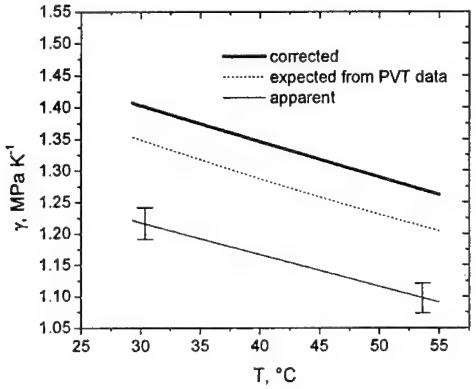

Figure 15. Thermal pressure coefficient vs temperature from the data shown in Figure 14. Error bars of 25 kPa/K in apparent curve show the precision in γ determination. The dotted line is expected curve based on literature PVT data[23].

Measurements During Thermoset Cure in the Spherical Pressure Vessel

The model epoxy resin (DGEBA/TMAB) was used to provide an example of the performance of the spherical pressure instrument during thermoset cure. After filling the vessel with the epoxy resin, the resin was degassed and the air was removed from the vessel. The vessel was then sealed by flattening the tip of the filling stem with a pipe crimping tool and then polymerizing the resin in the top part of the stem by inserting the stem for 10 minutes into a soldering iron finger set to 350°C. An alternative and easier way to seal the vessel is to place a threaded end cap (Swagelok Company) at the end of the filling stem, as was done for the oil measurements and as is done for the tubular pressure vessel. However with this method it is difficult to control the free volume left in the stem of the spherical pressure vessel and, therefore, is difficult to control the temperature at which compressive stresses start to build up.

The isotropic stress development in the epoxy resin during a typical cure cycle was shown in our second annual report and we do not reshow that data. Several important points from those experiments, however, are reiterated. During the cure cycle, the material became compressed during the initial heating and then these stresses were relieved as the material cured. However, once the stresses became tensile, microfailure was observed and only small tensile stresses (< 3 to 5 MPa) remained at the end of the isothermal cure. When we sealed vessels at lower temperatures, compressive stresses started to develop much earlier and, in some cases, the stress increased beyond the yield stress of the vessels (30 to 35 MPa). Hence, the tubular pressure vessel method which can be used to over 350 MPa was developed in order to measure the cure-induced stresses under compression for the entire conversion range.

The isotropic stress development during an isothermal cure at 140°C is shown in Figure 15 for the same epoxy system. Although this figure was also shown in the previous report, we repeat it here because we have further analyzed the data and because of the importance of the findings, which were corroborated by experiments on the thick-walled tube which will be discussed subsequently. When the temperature is kept constant, all stresses develop solely due to the cure process. After about 50 min from the beginning of the isotherm the cure shrinkage relieves the compressive stresses in the vessel. Tensile stresses start to build up rapidly at 73 min at a conversion of approximately 0.6 as estimated from the measured heat flow. The time-temperature-transformation (TTT) cure diagram of this system[26] suggests that gelation of the

thermoset happens after 63 min of cure at 140°C at a conversion of 0.58. Thus the gelation triggers the development of tensile stresses, as expected. These tensile stresses reached 2 MPa (less than 1 MPa in the second experiment) and are subsequently released by microfailure of the resin. The tensile cure stresses after microfailure continue to build up more slowly, reaching 1.5 MPa (1.2 MPa in the second experiment) at the end of the isotherm.

According to the TTT diagram[26] vitrification of this epoxy at 140°C should happen after 280 min from the beginning of cure (at a conversion of 0.97). This is in agreement with the measured heat flow, which at that time reaches its steady state value because the reaction has slowed to below the detectable limit. The area under the heat flow curve during the isotherm equals 370 ± 30 J/g, which is in a good agreement with the expected 381 J/g heat release during cure of this epoxy[27].

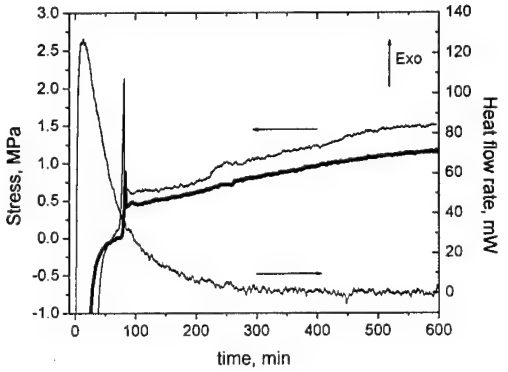

Figure 16. Isotropic stress development and heat flow rate during an isothermal cure of epoxy at 140°C in the sperhical pressure vessel. Thick and thin stress curves correspond to two different measurements.

We anticipated considerably larger tensile stresses during cure based on previous measurements of a different resin using a conventional long hollow aluminum cylinder as a constraint.[21] In that work, cure-induced tensile stresses of 21 MPa were reported. Various steps (chemical etching of the inner surface of the vessel, use of titanium spherical vessel) taken to increase adhesion between the resin and the vessel did not result in higher tensile stresses during isothermal cure. It appears that for the present system, the resin network after gelation is not strong enough to support high tensile stresses. This fact is not included in recent modelling of isotropic residual stresses.[21,28,29]

The Thick-Walled Tube: Isotropy, Calibration and Test Results

Stress Isotropy in the Tubular Geometry

The development of the present thick-walled tube method evolved from our attempts to overcome the disadvantage of thin-walled tubes that are commonly used to measure isotropic stress development in thermosets[19-21] and the disadvantage of the spherical pressure vessel which yielded at 30 to 35 MPa. In the present section we show that, in fact, the thin-walled tubes do not provide a ready means of applying and measuring isotropic stresses to solid materials. Figure 17 shows an example of the stress anisotropy in a resin constrained in conventional thin-walled tubes; positive values correspond to tensile stresses. Measurements were taken on cooling after cure, and show that the apparent thermal pressure coefficient γ obtained from the slope of the stress versus temperature curves for the axial and hoop measurements differ by a factor of

2.5. Apparent thermal pressure coefficients obtained from the axial and hoop measurements are closer as the walls become thicker. For example, Figure 17b shows less anisotropy of the stress field than Figure 17a. The values of the thermal pressure coefficients also become larger for the thicker wall tube, revealing the influence of the compliance of the tube on the measured thermal pressure coefficient.

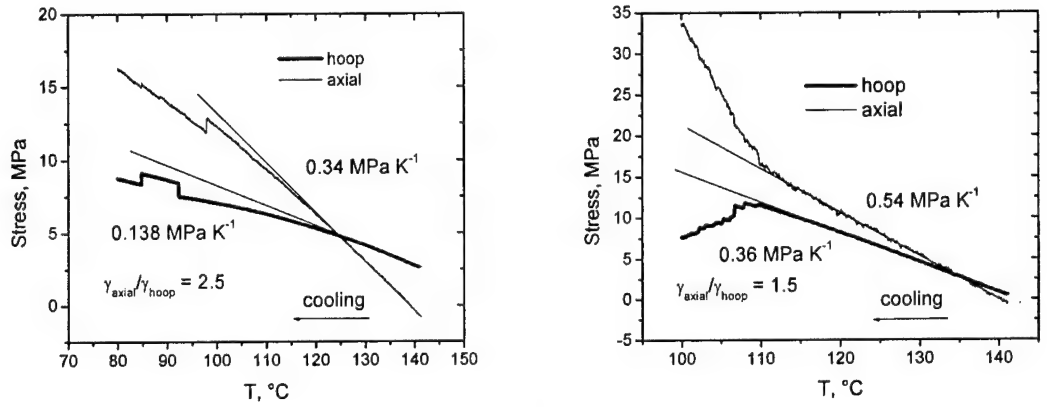

a) b)

Figure 17. Stress development during cooling of an epoxy resin after 10 hours cure at 140°C. The two curves (thick and thin) correspond to hoop and axial stresses. The values for the apparent thermal pressure coefficients γ are shown. a) aluminum tube with 0.25 in outer diameter and 0.01 in wall thickness; failure occurs below 100°C. b) aluminum tube with 0.25 in outer diameter and 0.035 in wall thickness; failure occurs below 110°C.

To test the stress isotropy in our thick-walled vessel, we examined the development of tensile stresses during cooling for sucrose benzoate as we did for the spherical pressure vessel. Again, the vessel was left open such that stresses only developed upon vitrification. Similar to the results shown in Figure 13 for the spherical pressure instrument, the sucrose benzoate vitrified at approximately 65 to 70°C and, subsequently, tensile stresses built up to 10 MPa until failure occurs at 57°C, relieving most of the stresses. Note that in Figure 18, the axial stress curve is shifted down by 4 MPa for clarity. Before failure the stress versus temperature curves from the hoop and axial gages are identical within experimental uncertainties, indicating good isotropy of the stress field.

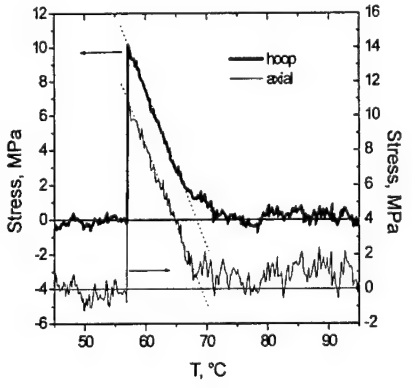

Figure 18. Hydrostatic stresses vs temperature in the tube filled with sucrose benzoate during cooling at 1 K/min. The two stress curves correspond to stresses in hoop and axial directions of the tube.

Thermal Pressure of a Known Fluid in the Thick-Walled Tube

The thermal pressure of di-2-ethylhexyl sebacate, confined in the tube, was measured to check the accuracy of the method using the same methodology as was used for the spherical pressure instrument. The development of thermally induced stresses in the tube during cooling at 0.5 K/min is shown in Figure 19. As in the case of the spherical pressure vessel, the measured γ_{app} was determined by the fitting stress/temperature curve in Figure 19 by a second order polynomial in the temperature range from 40°C to 150°C and taking the temperature derivative of that fit, which results in a straight line in the γ_{app} temperature dependence. Use of a higher order polynomial increases the uncertainties in the γ_{app} determination. However, since the straight line may lack some features of the actual γ_{app} temperature dependence, we also took 20 K segments of stress/temperature curve with 10 K interval and determined their slope from a linear fit. Both values of γ_{app} are shown in Figure 20 along with corrected and expected values, the latter of which are based upon PVT data from Sane and Knauss[23] calculated for the temperature-pressure profile of the experiment. After correcting for the thermal expansion and for the tube compliance, the measured values agree to within 12 kPa/K or within 1% of the expected values in a temperature range from 100°C to 150°C. Below 100°C the measured values become gradually lower than expected. There are several possible explanations for this discrepancy: i) at low values of pressure the tube may be "softer" than estimated (i.e., K_v is lower); ii) a small air volume may have been trapped during closing lower the actual thermal pressure coefficient especially at lower pressures; iii) the expected thermal pressure coefficient obtained from Knauss' data may be incorrect because we had to determine γ as the ratio of two derivatives, $\gamma = -\left(\frac{\partial V}{\partial T}\right)_P \Big/ \left(\frac{\partial V}{\partial P}\right)_T$, making it sensitive to the choice of the material function *V(T,P)* used to fit the literature PVT data. It should be noted that the results for the thermal pressure coefficient in Figure 15 from the spherical pressure vessel cannot be directly compared to those in Figure 20 for the tubular pressure vessel because the value of γ depends on pressure and temperature, and the pressure is not the same for a given temperature in the two measurements (as can be seen by comparing Figures 14 and 19).

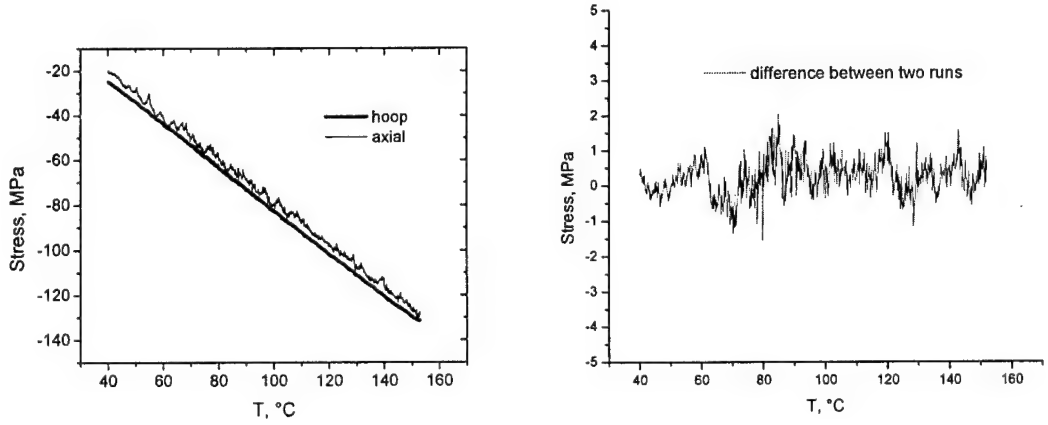

Figure 19. Thermally-induced compressive stress in the tube filled with di-2-ethylhexyl sebacate oil vs temperature during cooling with 0.5 K/min.

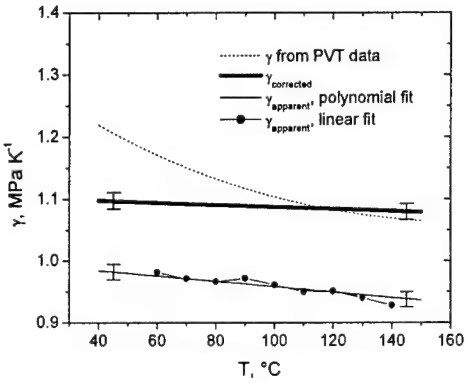

Figure 20. Thermal pressure coefficient vs temperature from the data shown in Fig. 19. Error bars of 12 kPa/K in the apparent curve show the precision in γ determination. The dotted line is the expected curve based on the PVT data from ref. 23.

Measurements During Thermoset Cure in the Tubular Pressure Vessel

The model epoxy resin DGEBA/TMAB was used to provide an example of the performance of the instrumented thick-walled tube during thermoset cure. The model epoxy resin was used for measurements because its curing reactions do not change with cure temperature (unlike the BMI model resin), and hence, the effects of cure temperature independent of changes in cure chemistry can be evaluated. Filling was performed in a manner similar to that described for the spherical pressure vessel except that the tube was closed with a threaded end cap. For some experiments, the vessel was left open to better simulate cure in a composite in which the resin is unconstrained prior to gelation.

The isotropic stress development in the epoxy resin constrained in a closed thick-walled tube during a typical cure cycle is shown in Figure 21; Figure 21a shows the results as a function of time, whereas Figure 21b shows the results as a function of temperature. The cure history as a function of time is also shown in Figure 21a. Positive and negative values of isotropic stress correspond to tension and compression, respectively. At the beginning of the experiment there was an initial compressive stress built up during sealing of the tube. On heating the epoxy resin expands increasing the value of compressive stress. At approximately 110°C the cure reaction begins, which leads to shrinkage. The competing thermal expansion and cure shrinkage balance one another at approximately 125°C. On further heating, the cure shrinkage dominates the thermal expansion and the compressive stresses decrease. Hoop and axial stresses were the same until the resin solidified during isothermal cure. At that point, it appears that cure shrinkage in the gelled resin relieves compressive hoop and axial stresses differently, resulting in different values of residual compressive stresses at the end of the cure. Such differences were observed in all experiments. In spite of the difference in absolute values of hoop and axial tensile stresses at the end of cure, the values of apparent thermal pressure coefficient obtained during cooling after cure are the same for hoop and axial directions. On cooling the resin shrinks and the tensile stresses built up until failure in the resin or debonding between the resin and the tube wall occurred below 90°C at hoop stresses of approximately 20 MPa. In the experiment depicted in Figure 21, cure shrinkage relieved approximately 150 to 200 MPa of the compressive stresses, if one takes into account thermal expansion up to 160°C. These facts are not included in recent modeling of isotropic residual stresses.[21,28,29]

The values of apparent thermal pressure coefficients, calculated from the slope of the stress vs temperature curves during heating of uncured resin and cooling of the cured resin, are shown in Fig. 21b. Interestingly, the value of thermal pressure coefficient of the uncured resin is larger than that of the cured resin. This fact is not included in previous models of isotropic stress development in thermosetting materials,[21,29,30] although recent work from the present laboratory includes such differences and comments upon their importance.[28]

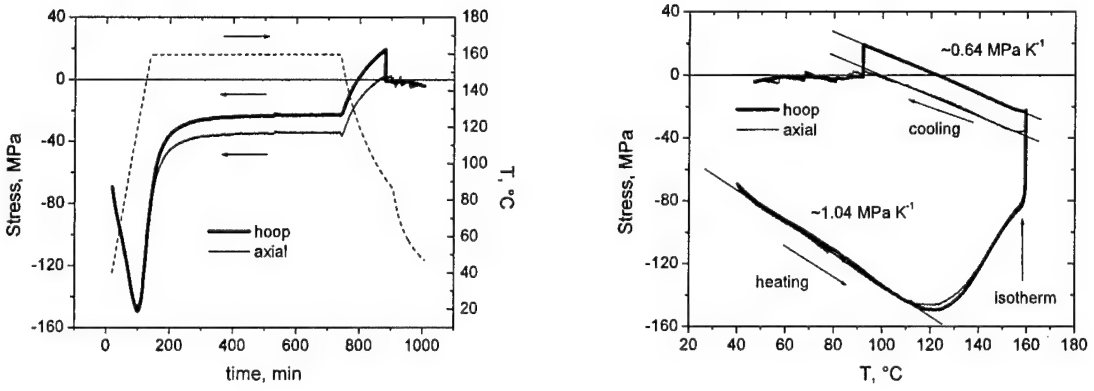

a) b)

Figure 21. Stress development in a closed thick-walled tube during a heat-hold-cool cure cycle for an epoxy resin. a) Stress vs time curves and temperature profile (dashed line). b) Stress vs temperature curves. Apparent values for the thermal pressure coefficient are indicated. Thick and thin lines correspond to stresses in hoop and in axial directions, respectively.

The closed instrumented tube allows us to examine the effects of cure shrinkage on residual stress development over the entire range of conversion since the isothermal portion of the cure (and post-cure if any) can be carried out with the resin in a state of compression. As shown in Figures 16 and 21, if the initial compression (due to heating of the constrained resin) is not great enough, the stresses become tensile during cure and microfailure occurs limiting the magnitude of the tensile stress at the end of the isothermal cure. To examine whether the tensile stresses that could be maintained by the curing gel depended on cure temperature and whether microfailure in the gel effected the thermal pressure coefficient, we performed two-step cure studies in open tubes and varied the temperature of the first cure step. We performed the second step at 160 °C to ensure complete conversion at the end of the two-step cure for each experiment. Figure 22 shows tensile stress developed during the first cure step as a function of time for cure temperatures of 100, 120, 140 and 160 °C. In all cases, microfailure is observed to occur, and at the highest temperatures, the stress at the end of the first cure step is initially zero. For the material cured at 100 °C, however, the stress build-up is significantly higher, reaching 7 MPa at the end of the first cure step in spite of the fact that some microfailure was still observed. Interestingly, the value of the thermal pressure coefficient for the glass γ_g is found to be a function of the temperature of the first cure step (T_{c1}), presumably because the degree of microfailure in the gel depends on the temperature and this, in turn, affects the final state and properties of the material. The results for two experiments at each cure temperature (except at 160 °C where only one experiment has been performed to date) are shown in Table 1. Two points are worth noting: first, the value of the thermal pressure coefficient decreases with increasing T_{c1}, and second, the microfailure incurred during the first cure step results in an

anisotropic state of the resin affecting the reproducibility of the thermal pressure coefficient calculated only from the hoop stress. For example, for T_{c1} = 100 °C, the values of γ_g for the two experiments agree to better than 7 % and the values change less than 5% when the axial component is included in the calculation. On the other hand, at 120 and 140 °C, the values from the two separate experiments are much more disparate when calculated from only the hoop stresses, but they agree when the axial component is included in the calculation indicating that at these higher cure temperatures, the microfailure observed in Figure 18 results in anisotropy of the stress field. These two observations are very significant for modeling isotropic stress development during cure of thermosetting resins and has not been reported in the literature before to the best of the authors' knowledge.

Table 1. The apparent thermal pressure coefficient in the glass γ_g after a two-step cure at cure temperature T_{c1} followed by complete conversion at T_{c2} = 160 °C. The values reported were taken from the slope of the stress vs. temperature curves between 120°C and 140°C. Except for the cure at 160°C, two samples were cured at each cure temperature with both values reported.

T_{c1}, °C	γ_g from hoop stress, MPa/K	γ_g from hoop and axial stresses, $(2\sigma_{hoop}+\sigma_{axial})/3$, MPa/K
100	0.86, 0.92	0.88, 0.96
120	0.37, 0.63	0.69, 0.77
140	0.14, ~0	0.36, 0.39
160	~0.05	~0.05

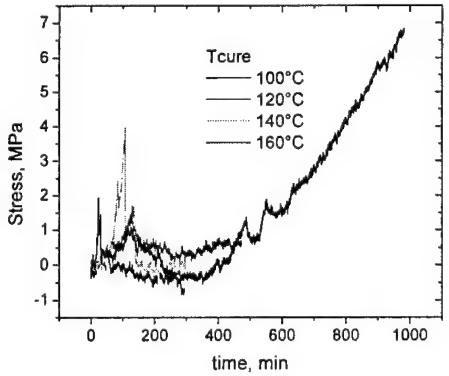

Figure 22. Stress development in an open thick-walled tube during the first step of a two-step cure cycle for an epoxy resin as a function of time for four different values of the cure temperature.

Results of Thermogravimetric Experiments for the BMI/SOC Resin

As previously mentioned, thermogravimetric analysis (TGA) was performed on the BMI/SOC resin to determine if resin volatility was the cause of lack of reproducibility, the unexplained very low thermal pressure coefficients, and the lack of SOC signature in the FTIR cure data. Uncured resin samples were loaded at room temperature. A ramp was performed at 5 K/min to 140 °C, which was the mixing temperature for the resin. After a hold of 30 minutes at 140 °C to simulate mixing, the material was ramped to 300 °C to simulate the ramp to the cure temperature. TGA experiments were run on the all of the individual components of the BMI/SOC resin, i.e., on the SOC comonomer alone, on Matrimid 5292A alone, on Matrimid

5292 B alone, as well as on various mixtures of these components with and without catalyst. For clarity, in Figures 23, 24, and 25, we only show the results for the SOC comonomer alone, for the BMI/SOC resin system (with the SOC catalyst) and for the Matrimid 5292A/5292B resin system (termed BMI). Figure 23 shows the results of the ramp to 140 °C; Figure 24, the results

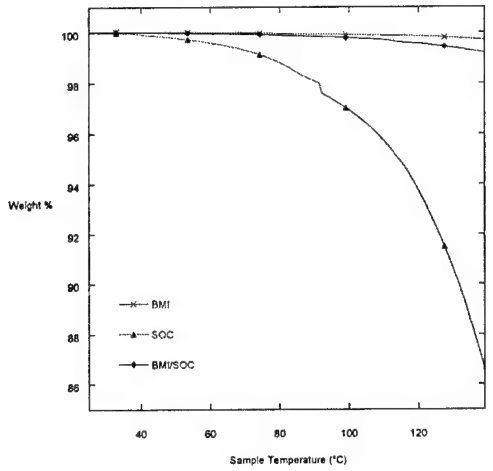

Figure 23. Weight loss as a function of sample temperature for the three resins indicated during a temperature from room temperature to 140 °C at 5 K/min. In order to form homogeneous solutions, the BMI and BMI/SOC resin samples where mixed at 140 °C before the TGA experiment for approximately 15 minutes.

of the isothermal hold at 140 °C for 30 mintues; and Figure 25, the results of the ramp from 140 to 300 °C. Our findings show that the SOC comonomer is substantially more volatile than any of the other components and that less than 25 % of it remains after 30 minutes at 140 °C and less than 10 % remains after the ramp to 300 °C. In the BMI/SOC mixture, there is significantly less

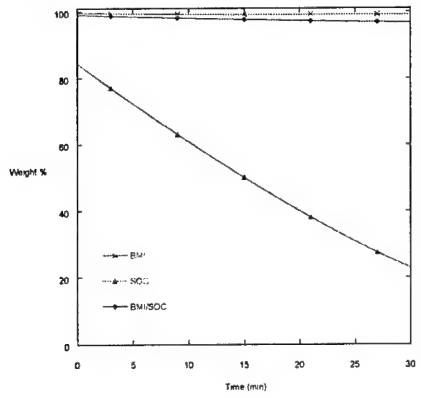

Figure 24. Weight loss as a function of time during a 30 minute isotherm at 140 °C performed after completion of the initial ramp from room temperature to 140 °C (shown in Figure 19). This step simulates the mixing step for the resins.

weight loss since the SOC comprises only 9 % by weight of the total system. However, the weight loss relative to the commercial BMI system is significant, being four times greater at approximately 4% after 30 minutes at 140 °C. The TGA results indicate that the reason for our difficulty in working with this system is due to the relatively high volatility of the SOC comonomer. In addition, its high volatility preclude its being a feasible candidate for resins used in structural composite applications.

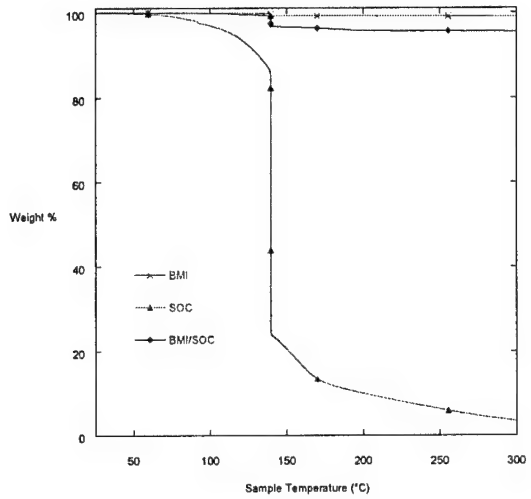

Figure 25. Weight loss as a function of temperature for a ramp from 140 °C to 300 °C at 5 K/min; the ramp was performed after the isothermal hold shown in Figure 20. This step was used to simulate the ramp to cure temperature.

References

1. S. L. Simon, G. B. McKenna, and O. Sindt, *J. Appl. Polym. Sci*, **76**, 495, (2000).
2. J. D. Ferry, "Viscoelastic properties of polymers"; John Wiley and Sons: New York, 1980.
3. M. L. Williams, R. F. Landell and J. D. Ferry, *J. Am. Chem. Soc*, **77**, 3701, (1955).
4. D. J. Plazek, *J. Polym. Sci: Part A-2*, **4**, 745, (1966).
5. A. Lee and G. B. McKenna, *Polymer*, **29**, 1812, (1988).
6. T. G. Fox, *Bull. Am. Phys. Soc*, **1**, 123, (1958).
7. E.A. DiMarzio, *J.Res.Natl.Bur.Std., Sect.A, 68A*, **611**, (1964).
8. A. Hale, C. W. Macosko and H E. Bair, *Macromolecules*, **24**, 2610, (1991).
9. D. R. Miller and C. W. Macosko, *Macromolecules*, **9**, 200, 1976.
10. D. R. Miller and C. W. Macosko, *Macromolecules*, **9**, 206, 1976.
11. D. W. Van Krevelen, "*Properties of Polymers. Correlations with Chemical Structure*," Elsevier, Amestrdam, 1972.
12. J. E. Mark, "Physical properties of polymers handbook," J. E. Mark, 1996.
13. Chuk Leung, PolyComp, private correspondence.
14. R. J. Morgan, E. E. Shin, B. Rosenberg and A. Jurek, *Polymer*, **38**, 639, (1997).
15. G. B. McKenna and R. W. Penn, *Polymer*, **21**, 213, (1980).

16. G. B. McKenna and R. W. Penn, *J. Biomedical Mater. Res*, **14**, 689, (1980)
17. J. M. Crissman and McKenna, *J. Polym. Sci: Part B: Poly.Phys*, **25**, 1667, (1987).
18. H. T. Hahn, ASTM STP 674, 383 (1979)
19. A. R. Plepys and R. J. Farris, Polymer, **31**, 1992 (1990).
20. D. B. Adolf and R. S. Chambers, Polymer, **39**, 5481 (1997).
21. P. Prasatya, G. B. McKenna, and S. L. Simon, J. Comp. Mat., **35**, 826 (2001).
22. General information in *Strain Gages for Stress Analysis*, BLH Electronics, catalog-No. 215-A, available at http://www.sr4.com.
23. S.B. Sane and W.G. Knauss, Mech. Time-Depend. Mat., **5**, 293 (2001).
24. P. Zoller and D.J. Walsh, *Standard Pressure-Volume-Temperature Data for Polymers*, (Technomic Publishing Company, Lancaster, 1995).
25. R.A. Orwoll and P.J. Flory, J. Am. Chem. Soc., **89**, 6814 (1967).
26. G. Wisanrakkit and J.K. Gillham, J. Coat. Tech., **62**, 35 (1990).
27. S.L. Simon and J.K. Gillham, J. Appl. Polym. Sci., **46**, 1245 (1992).
28. M. Alcoutlabi, G. B. McKenna, and S. L. Simon, J. Appl. Polym. Sci., **88,** 227 (2003).
29. D. B. Adolf, J. E. Martin, R. S. Chambers, and S. N. Burchett, J. Mater. Res., **13**, 530 (1998).
30. D. Adolf and J. E. Martin, J. Comp. Mat., **30**, 13 (1996).

APPENDIX

A. Project Accomplishments

- Modeled the development of isotropic residual stresses in a novel SOC/BMI thermosetting material. The volume versus conversion and the T_g versus conversion relationships were estimated using the group contribution methods of van Krevelen and using statistical recursive theory.
- Performed a parametric analysis and determined the effect of various parameters on the isotropic residual stresses, including cure cycle parameters and material parameters.
- Developed an isotropic stress "bomb" method for measuring the thermal pressure coefficient $\gamma=\alpha K$ in the liquid and glassy states of thermosetting resins and made measurements for several thermosetting systems, including the novel BMI/SOC resin.
- Performed thermogravimetric measurements of the BMI/SOC resin system and established that the volatilization of the SOC component makes clear that this resin system is not applicable for structural composites.
- Developed an instrument for measuring isotropic stress development in curing resins having a thick-walled tubular geometry using a lock-in amplifier technique to measure strain. The method has advantages over the spherical pressure vessel geometry in that thermal pressures of over 300 MPa can be measured. In addition, the cure stresses can be quantified over the entire conversion range by keeping the resin in a compressive stress state throughout cure.
- Completed the calibrations, reproducibility studies, and test measurements on a fluid with known PVT properties for both the spherical and tubular isotropic stress instruments in order to demonstrate the range and accuracy of the measurements.
- Completed measurements and analyses of a model epoxy resin in both the tubular and spherical isotropic stress instruments. The model epoxy resin was used for measurements because its curing reactions do not change with cure temperature; hence, the effects of cure temperature independent of changes in cure chemistry can be evaluated.

B. Program statistics

(1) Number of PI and Co-PIs involved in the research project: 2

Gregory B. McKenna
Sindee L. Simon

(2) Number of Post Doctoral researchers supported on this grant by AFOSR: 4

Mustafa Iza
Mikhail Merzliakov
Mataz Alcoutlabi
Paul A. O'Connell (appointed as research professor in middle of granting period)

(3) Number of graduate students supported on this grant by AFOSR: 2

Stephen A. Hutcheson
Yan Meng

(4) Other researchers supported on this grant by AFOSR: 1

Neil McFerran

(5) Peer reviewed publications by PIs in the last 12 month period:

9 refereed journal articles (listed below)
7 refereed conference proceedings (listed below)

Refereed Journal Articles (9)

1. S. L. Simon, P. Bernazzani, and G. B. McKenna, "Effects of Freeze-Drying on the Glass Temperature of Cyclic Polystyrenes," Polymer, **44**, 8025-8032 (2003).
2. D. Huang, S. L. Simon and G. B. McKenna, "Equilibrium Heat Capacity of the Glass-Forming Poly(α-methyl styrene) Far Below the Kauzmann Temperature: The Case of the Missing Glass Transition," Journal of Chemical Physics, 119 (7), 3590 - 3593 (2003).
3. I. Echeverria, P. L. Kolek, D. J. Plazek, and S. L. Simon, "Enthalpy Recovery, Creep and Creep-Recovery Measurements during Physical Aging of Amorphous Selenium," Journal of Non-Crystalline Solids, 324/3, 242 - 255 (2003).
4. T. Rajagopalan, J. Sun, B. Lahlouh, J. A. Lubguban, D. Huang, N. Biswas, S. L. Simon, S. Gangopadhyay, A. Malikarjun, H. C. Kim, W. Volksen and R. D. Miller, "Supercritical Carbon Dioxide Extraction of Porogens for the Preparation of Ultralow-Dielectric-Constant Films," Applied Physics Letters, 82 (24), 4328 - 4330 (2003).
5. M. Alcoutlabi, G. B. McKenna, and S. L. Simon, "Analysis of the Development of Isotropic Residual Stresses in BMI/SOC Thermosetting Resin for Composite Materials," Journal of Applied Polymer Science, 88 (1), 227 - 244 (2003).
6. G.B. McKenna, "Mechanical Rejuvenation in Polymer Glasses: Fact or Fallacy?," J. Phys. Cond. Matter, **15**, S737-S763 (2003).
7. Y. Zheng and G.B. McKenna, "Structural Recovery in a Model Epoxy Comparison of Responses after Temperature and Relative Humidity Jumps," Macromolecules, **36**, 2387-2396 (2003).

8. G.B. McKenna, "Status of Our Understanding of Dynamics in Confinement: Perspectives from Confit 2003," Europ. Phys. J. E., **12**, 191-194 (2003).
9. Y. Zheng, R.D. Priestley and G.B. McKenna, "Physical Aging of an Epoxy Subsequent to Relative Humidity Jumps through the Glass Concentration," J. Polym. Sci., B. Polym.Phys.,(In press).

Refereed Proceedings (7)

1. Y. Zheng and G.B. McKenna, "Structural Recovery in a Model Epoxy after Rapid Relative Humidity Changes," Proceedings 61st Annual Technical Conference, ANTEC 2003, Society of Plastics Engineers, 1620-1623 (2003).
2. A. Flory and G.B. McKenna, "The Influence of Finite Step Time on the Measurement of the Viscoelastic Response Functions," Proceedings 61st Annual Technical Conference, Society of Plastics Engineers, ANTEC 2003, 1971-1975 (2003).
3. X.F. Shi and G.B. McKenna, "Mechanical Hole Burning Spectroscopy: A Comparison of Two Scenarios," Proceedings 61st Annual Technical Conference, ANTEC 2003, Society of Plastics Engineers, 947-951 (2003).
4. M. Merzlyakov, Y. Meng, S.L. Simon and G.B. McKenna, "Evaluation of Different Methods of Measurement for the Isotropic Stress Development in Curing Thermosets," Proceedings 61st Annual Technical Conference, ANTEC 2003, Society of Plastics Engineers, 1898-1902 (2003).
5. S. L. Simon, T. F. Wiesner, and L. R. Heinze, "Program Improvements Resulting from Completion of One ABET 2000 Assessment Cycle," Proceedings of the Annual Meeting of the American Society of Engineering Education. Paper 1638, Session 3413, June 22-25, 2003.
6. P. Bernazzani, S. L. Simon, D. J. Plazek and K. L. Ngai, "Depression of Tg in Polystyrene by Freeze-Drying," Society of Plastics Engineers, Annual Technical Meeting Proceedings, SPE ANTEC 2003, 1987 - 1991 (2003).
7. B. Lahlouh, T. Rajagopalan, J. A. Lubguban, N. Biswas, S. Gangopadhyay, J. Sun, D. Huang, S. L. Simon, H. C. Kim, W. Volksen and R. D. Miller, "Creating Nanoporosity by Selective Extraction of Porogens using Supercritical Carbon Dioxide/Cosolvent Processes," Materials Research Society Symposium Proceedings no.766, "Materials, Technology and Reliability for Advanced Interconnects and Low-k Dielectrics," 291-296 (2003).

(6) Number of publications in the last 12 months that acknowledge AFOSR support:

Refereed Journal Articles Acknowledging AFOSR Support (1 published, 1 submitted, 2 in preparation)

1. M. Alcoutlabi, G. B. McKenna*, and S. L. Simon*, "Analysis of the Development of Isotropic Residual Stresses in BMI/SOC Thermosetting Resin for Composite Materials," Journal of Applied Polymer Science, 88 (1), 227 - 244 (2003).
2. M. Merzlyakov, Y. Meng, S.L. Simon and G.B. McKenna, "An Instrumented Sphere Method for Measuring Thermal Pressure in Fluids and Isotropic Stresses and Reaction Kinetics in Thermosetting Resins," Rev. Sci. Instr., (submitted 2003).

3. M. Merzlyakov, S.L. Simon and G.B. McKenna, "An Instrumented Thick-Walled Tube Method for Measuring Thermal Pressure in Fluids and Isotropic Stresses in Thermosetting Resins, to be submitted to Rev. Sci. Instr.
4. M. Merzlyakov, G.B. McKenna and S.L. Simon, "Isotropic Stress Development in Curing Thermosets," to be submitted to Composites, Par A. Applied Science and Manufacturing.

Refereed Proceedings acknowledging AFOSR Support (2)

1. M. Merzlyakov, Y. Meng, S.L. Simon and G.B. McKenna, "Evaluation of Different Methods of Measurement for the Isotropic Stress Development in Curing Thermosets," Proceedings 61st Annual Technical Conference, ANTEC 2003, Society of Plastics Engineers, 1898-1902 (2003).
2. M. Merzlyakov, G.B. McKenna and S.L. Simon, "Effect of Cure Cycle on Residual Stress Development in Thermosetting Materials, ANTEC 2004, Society of Plastics Engineers (in press).

(7) Awards and Honors received by the PI and Co-PI (life-time received)

Gregory B. McKenna

- Vice-Chair Gordon Conference on "Elastomers." Will serve as chair for 2005 meeting (Elastomers, Networks and Gels).
- Received Outstanding Service Award, Society of Plastics Engineers, Polymer Analysis Division, May 2002.
- Received North American Thermal Analysis Society (NATAS) award for outstanding achievement in thermal analysis (sponsored by Mettler-Toledo), September 2001.
- Best Paper award from the American Society of Composites, Polymer Matrix Division, 2000 (awarded September 2001).
- Received Society of Plastics Engineers 2000 SPE International Research Award (in memory of John C. Moricoli), May 2000.
- Editor Journal of Polymer Science, Polymer Physics Edition, 2002-present.
- Associate Editor Journal of Polymer Science, Polymer Physics Edition, 2000-2002.
- Awarded John R. Bradford Chair in Engineering, Texas Tech University, 1999-present.
- Awarded Russell Severance Springer Professorship (Visiting) for Academic Year 1999-2000, University of California Berkeley, Department of Mechanical Engineering.
- Elected Fellow of the Society of Plastics Engineers, May, 1998.
- Member of Editorial Review Board, Journal of the Mechanics of Time Dependent Materials, 1997-present.
- Received Society of Plastics Engineers Best Paper Award, EPSDIV, ANTEC 1996.
- Member of Editorial Review Board, Composites Engineering, 1994.
- Member of Editorial Review Board, Journal of Polymer Science, Polymer Physics Edition, 1992-2000.
- Received U.S. Department of Commerce Silver Medal Award for Outstanding Federal Service in December, 1992.
- Member of Editorial Review Board, Journal of Rheology, 1990-present.

- Received the Edward U. Condon Award for Distinguished Achievement in Writing, December, 1989: "Glass Formation and Glassy Behavior, " in Comprehensive Polymer Science: Vol. 2. Polymer Properties, ed. By C. Booth and C. Price, Pergamon, Oxford, 311-363 (1989).
- Elected Fellow of American Physical Society, March, 1989.
- Received U.S. Department of Commerce Bronze Medal Award for Superior FederalService in December, 1985.
- National Research Council/National Academy of Sciences Postdoctoral Fellowship at the National Bureau of Standards, 1976.
- Distinguished Graduate (Summa cum laude), U.S. Air Force Academy. (Third in class), 1970.

Sindee L. Simon

- Elected Vice President of the North American Thermal Analysis Society. Term begins January 1, 2004.
- Invited Speaker, Polymer Physics Gordon Conference, August 2004; invitation accepted.
- Fellow, North American Thermal Analysis Society (NATAS), Elected, September, 2003.
- Outstanding Service Award, Society of Plastics Engineers, Polymer Analysis Division, May 2002.
- Most Improved Newsletter, Society of Plastics Engineers, for PAD Review, May 2002.
- Best Paper award from the American Society of Composites, Polymer Matrix Division, 2000 (awarded September 2001).
- Plenary lecturer, North American Thermal Analysis Society Annual Meeting, 2000.
- DuPont Instruments Scholarship, 1990, administered by the Society of Plastics Engineers.
- Plastics Institute of America Supplemental Fellowship, 1988.
- Tau Beta Pi National Engineering Honor Society.
- Nellie P. Elliot Award, Yale University 1983, for outstanding scholastic and athletic achievements.
- Captain of Yale Women's Swim Team: 1981/82, 1982/83.
- All-American: 1982. Eleven Varsity Swimming Records (one of which stood for eleven years).